

Synthesis, spectral and thermal studies of the sodium salts of some Ru(III) complexes with quinolone antibiotics

Mihaela Badea¹ · Rodica Olar¹ · Luigi Silvestro² · Martin Maurer³ ·
Valentina Uivarosi⁴

Received: 30 October 2015 / Accepted: 12 October 2016
© Akadémiai Kiadó, Budapest, Hungary 2016

Abstract Solubilisation by salt formation is an effective method to increase the solubility of slightly soluble drugs, applied especially for the development of liquid formulations for parenteral administration. In the present study, this strategy is applied for new Ru(III) complexes with quinolone antibiotics, valuable for biological application such as anticancer activity. The parent compounds, formulated as $\text{RuCl}_3(\text{HL})_2(\text{DMSO})_m(\text{H}_2\text{O})_n$ (HL: pipemidic acid, norfloxacin, ciprofloxacin, ofloxacin, levofloxacin, enrofloxacin, enoxacin), were transformed in their corresponding soluble sodium salts with general formula $\text{Na}_2\text{-}_2\text{RuCl}_3(\text{L})_2(\text{DMSO})_m(\text{EtOH})_n(\text{H}_2\text{O})_p$. The sodium salts have been characterised by elemental analysis and some spectrometric methods (IR, UV–Vis, mass spectra). The thermal behaviour of these newly compounds was studied by simultaneous TG/DTG/DTA analysis, and it was evidenced a higher thermal stability compared to that of the parent compounds. The thermal transformations occur in two or three steps and comprise solvent (solvation or coordination) elimination as well as oxidative degradation

of quinolone derivatives. A mixture of ruthenium and sodium chloride was identified as final residue.

Keywords Quinolone derivative · Ruthenium(III) complex · Sodium salt · Thermal stability

Introduction

The increase in solubility of poorly soluble biological active compounds is a critical aspect related to the pharmacological screening of new chemical entities as well as in the design and development of pharmaceutical formulations [1]. Salts formation is the most common and effective method to increase the dissolution rate and solubility of acidic and basic drugs [2]. The essential condition for salt forming is the presence of ionisable groups in the chemical structure. The advantages of using salts are represented by the enhanced stability and solubility in polar solvents (mainly water). More than half of the solid-state pharmaceutical active substances used nowadays are salts (approx. 75 % are cationic salts and 25 % anionic salts). The most used counterion for the anionic substances is Na^+ , followed by Ca^{2+} , K^+ and Mg^{2+} [3].

The synthetic strategy for obtaining soluble salts was applied for some ruthenium (III) complexes with antitumor or antimetastatic activity. The first type of complexes, obtained by Keller and Keppler [4], is represented by ruthenium (III) anionic complexes with N donors heterocycles as unidentate ligands and most successful of its have the formula $\text{trans-}[\text{RuCl}_4(\text{L})_2]^-$, where L is imidazole (KP418) or indazole (KP1019 and KP1339), and the counterion is $(\text{LH})^+$ or Na^+ .

KP1019 and KP1339 proved activity in the inhibition of platinum resistant rat colorectal carcinomas [5]. The major

✉ Valentina Uivarosi
uivarosi.valentina@umf.ro

¹ Department of Inorganic Chemistry, Faculty of Chemistry, University of Bucharest, 90-92 Panduri St., Sector 5, 050663 Bucharest, Romania

² Pharma Serv. International SRL, 52 Sabinelor St., Sector 5, 050853 Bucharest, Romania

³ 3S-Pharmacological Consultation & Research GmbH, 1 Koenigsbergerstrasse, 27243 Harpstedt, Germany

⁴ Department of General Inorganic Chemistry, Carol Davila University of Medicine and Pharmacy, 6 Traian Vuia St., 020956 Bucharest, Romania

disadvantage of KP1019 in its development as anticancer agent represented by the poor water solubility was solved by transformation in sodium salt that results in an increase of 35 times of the solubility compared to the parent compound [6].

The second class of ruthenium (III) compounds consists in dimethyl sulfoxide-ruthenium (III) complexes with metastatic activity [7]. The most active compounds of this series are $\text{Na}\{\text{trans-}[\text{Ru(III)Cl}_4(\text{dmsO})(\text{Him})]\}$ (Him = imidazole) – NAMI, and $[\text{H}_2\text{im}][\text{trans-Ru(III)Cl}_4(\text{dmsO})(\text{Him})]$ – NAMI-A. NAMI, that belongs to a series of with general formula $\text{Na}[\text{trans-RuCl}_4(\text{R}_1\text{R}_2\text{SO})(\text{L})]$, where $\text{R}_1\text{-R}_2\text{SO}$ = dimethyl sulfoxide (DMSO) or tetramethylene sulfoxide (TMSO), L is a nitrogen donor ligand: imidazole (Im), oxazole (Ox), indazole (Ind), isoquinoline (Iq) [8], has an intense action on lung metastases [9–11]. Although the sodium salts of the anionic derivatives are slightly soluble in water, the reproducibility of their formulation is sometimes affected by the tendency to crystallise with DMSO and acetone molecules in variable proportions. Reproducible results are obtained with the LH^+ and NEt_4^+ salts, as it is NAMI-A.

This study is aimed to obtain soluble sodium salts of some ruthenium (III) complexes with quinolone antibiotics. The parent compounds, formulated as $\text{RuCl}_3(\text{HL})_2(\text{DMSO})_m(\text{H}_2\text{O})_n$ (HL: pipemidic acid, norfloxacin, ciprofloxacin, ofloxacin, levofloxacin, enrofloxacin, enoxacin) [12, 13] were transformed in their corresponding soluble sodium salts with general formula $\text{Na}_2\text{RuCl}_3(\text{L})_2(\text{DMSO})_m(\text{EtOH})_n(\text{H}_2\text{O})_p$ by neutralisation with sodium hydroxide. The obtained sodium salts were characterised by microanalytical, spectrometric methods (IR, UV–Vis, mass spectrometry) and thermal analysis. Having in view a possible application as drugs, the thermal analysis is required in order to develop proper drug conditioning and storage methods. As a result, the thermal analysis (TG, DTG and DTA) of the complexes was performed in order to establish temperature range of compounds thermal stability. This method also allowed us to confirm the proposed formulas of complexes and to elucidate the number and nature of the solvent molecules.

Experimental

Materials

All chemicals were purchased from Sigma-Aldrich, reagent grade and were used without further purification.

Synthesis of complexes

0.2 mmol of each parent neutral complex of general formula $\text{RuCl}_3(\text{HL})_2(\text{DMSO})_m(\text{H}_2\text{O})_n$ (HL: pipemidic acid, norfloxacin, ciprofloxacin, ofloxacin, levofloxacin,

enrofloxacin, enoxacin, respectively) was suspended in 10 mL of distilled water and neutralised with 0.2 mL of 2 M sodium hydroxide aqueous solution in a 1:2 molar ratio of complex to NaOH. The resulting solution was concentrated on the water bath near dryness, cooled on ice, and ethanol was added to yield a brown solid. The resulting precipitate was collected by filtration, washed with ethanol and air-dried.

Instruments

The chemical analyses were performed on a PerkinElmer PE 2400 analyser (for C, H, N, S) and a Shimadzu AA 6300 spectrometer (for Ru and Na).

IR spectra were recorded in KBr pellets with a FT-IR VERTEX 70 (Bruker) spectrometer in the range 400–4000 cm^{-1} .

Electronic spectra by diffuse reflectance technique, with MgO as standard, were recorded in the range 200–900 nm, on a Jasco V 650 spectrophotometer.

Mass spectrometry measurements were performed with THERMO PHINNIGAN MAT-900 mass spectrometer with FAB (THERMO-FINNIGAN) ionisation source operating in positive mode. Samples were dissolved in a matrix on nitrobenzyl alcohol. Molecular ions scanning range (m/z) was 0–1250.

The thermoanalytical curves (TG and DTA) were recorded using a Labsys 1200 SETARAM instrument, with a sample mass of 13–22 mg over the temperature range of 30–900 °C, using a heating rate of 10 K min^{-1} . The measurements were carried out in synthetic air atmosphere (flow rate 17 $\text{cm}^3 \text{min}^{-1}$) by using alumina crucibles. The calibration of TG equipment was run both with gold (m. p. 1064 ± 1 °C) and ultrapure $\text{CuSO}_4 \cdot 5\text{H}_2\text{O}$ (99.9 %) with a measurement error of 0.1 %.

The X-ray powder diffraction patterns were collected on a DRON-3 diffractometer with a nickel-filtered Cu K α radiation ($\lambda = 1.5418$ Å) in 2θ range of 5°–70°, a step width of 0.05° and an acquisition time of 2 s per step.

$\text{Na}_2[\text{RuCl}_3(\text{pip})_2(\text{DMSO})] \cdot \text{EtOH}$ (Hpip = pipemidic acid) (**1**) Analysis found: C, 39.54; H, 4.87; N, 13.96; S, 3.66; Ru, 10.15; Na, 4.28 %; calculated for $\text{C}_{32}\text{H}_{44}\text{Cl}_3\text{N}_{10}\text{Na}_2\text{O}_8\text{RuS}$: C, 39.12; H, 4.52; N, 14.26; S 3.26; Ru, 10.29; Na, 4.68 %. Reaction yield: 94 %.

$\text{Na}_2[\text{RuCl}_3(\text{enx})_2(\text{DMSO})] \cdot \text{EtOH} \cdot 3\text{H}_2\text{O}$ (Henx = enoxacin) (**2**) Analysis found: C, 38.18; H, 4.37; N, 9.98; S, 2.80; Ru, 9.12; Na 3.99 %; calculated for $\text{C}_{34}\text{H}_{50}\text{Cl}_3\text{F}_2\text{N}_8\text{Na}_2\text{O}_{11}\text{RuS}$: C, 38.15; H, 4.72; N, 10.47; S 2.94; Ru, 9.44; Na 4.29 %. Reaction yield: 79 %.

$\text{Na}_2[\text{RuCl}_3(\text{nf})_2(\text{DMSO})] \cdot \text{EtOH} \cdot \text{H}_2\text{O}$ (Hnf = norfloxacin) (**3**) Analysis found: C, 41.95; H, 4.14; N, 7.89; S, 3.48; Ru, 9.29; Na, 4.11 %; calculated for $\text{C}_{36}\text{H}_{48}\text{Cl}_3\text{F}_2\text{N}_6\text{Na}_2\text{O}_9\text{RuS}$:

C, 41.65; H, 4.69; N, 8.14; S, 3.10; Ru, 9.79; Na, 4.45 %. Reaction yield: 82 %.

$\text{Na}_2[\text{RuCl}_3(\text{cp})_2(\text{DMSO})] \cdot \text{DMSO} \cdot 2\text{EtOH}$ (Hcp = ciprofloxacin) (**4**) Analysis found: C, 43.81; H, 4.51; N, 7.22; S, 5.43; Ru, 8.31; Na, 3.42 %; calculated for $\text{C}_{42}\text{H}_{58}\text{Cl}_3\text{F}_2\text{N}_6\text{Na}_2\text{O}_{10}\text{RuS}_2$: C, 43.39; H, 5.04; N, 7.23; S 5.52; Ru, 8.69; Na, 3.96 %. Reaction yield: 85 %.

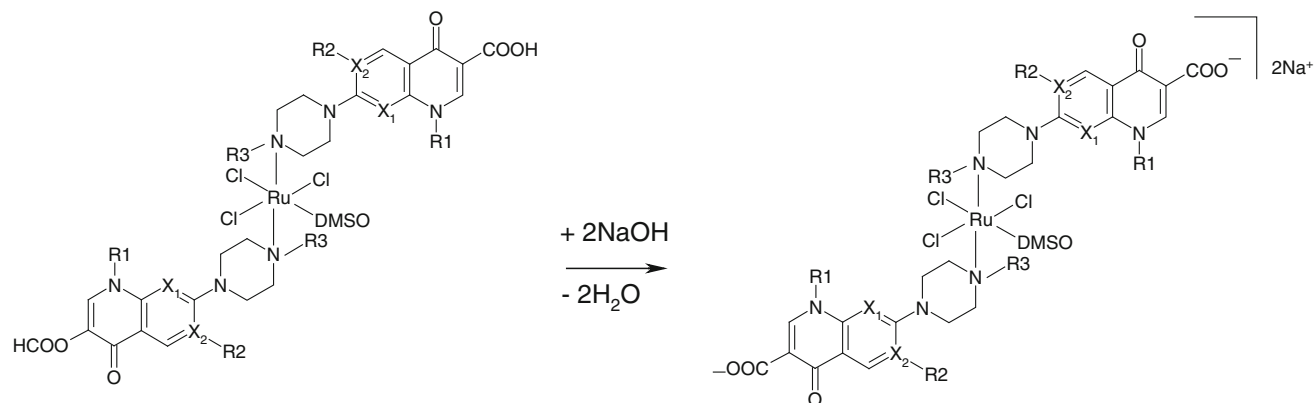
$\text{Na}_2[\text{RuCl}_3(\text{enro})_2(\text{DMSO})] \cdot 1.5\text{EtOH}$ (Henro = enrofloxacin) (**5**) Analysis found: C, 46.58; H, 4.82; N, 8.11; S, 2.87; Ru, 8.75; Na, 3.81 %; calculated for $\text{C}_{43}\text{H}_{57}\text{Cl}_3\text{F}_2\text{N}_6\text{Na}_2\text{O}_{8.5}\text{RuS}$: C, 46.26; H, 5.15; N, 7.52; S 2.87; Ru, 9.05; Na, 4.11 %. Reaction yield: 81 %.

$\text{Na}_2[\text{RuCl}_3(\text{of})_2(\text{DMSO})]$ (Hof = ofloxacin) (**6**) Analysis found: C, 43.76; H, 3.86; N, 7.50; S, 3.00; Ru, 9.31; Na, 3.97 %; calculated for $\text{C}_{38}\text{H}_{44}\text{Cl}_3\text{F}_2\text{N}_6\text{Na}_2\text{O}_9\text{RuS}$: C, 43.37; H, 4.22; N, 7.98; S 3.04; Ru, 9.60; Na, 4.37 %. Reaction yield: 92 %.

$\text{Na}_2[\text{RuCl}_3(\text{levof})_2(\text{DMSO})] \cdot 2\text{EtOH}$ (Hlevof = levofloxacin) (**7**) Analysis found: C, 44.28; H, 5.27; N, 7.71; S, 3.31; Ru, 8.44; Na, 3.64 %; calculated for $\text{C}_{42}\text{H}_{56}\text{Cl}_3\text{F}_2\text{N}_6\text{Na}_2\text{O}_{11}\text{RuS}$: C, 44.08; H, 4.94; N, 7.34; S 2.80; Ru, 8.83; Na, 4.02 %. Reaction yield: 95 %.

Results and discussion

In this paper, we report the preparation and physico-chemical characterisation of the sodium salts of some Ru(III) complexes with quinolone antibiotics. Synthesis of these derivatives was carried out according to a simple procedure as described in Scheme 1. The obtained salts have been formulated on the basis of chemical analysis, IR, electronic and mass spectra as well as thermal analysis as $\text{Na}_2\text{RuCl}_3(\text{L})_2(\text{DMSO})_m(\text{EtOH})_n(\text{H}_2\text{O})_p$, their formulation being described in Scheme 1 and Table 1. All these sodium salts are brown powders very soluble in water and slightly soluble or very slightly soluble in organic solvents as dimethylformamide, dimethyl sulfoxide, methanol and ethanol.





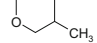
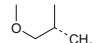
Scheme 1 General scheme for synthesis

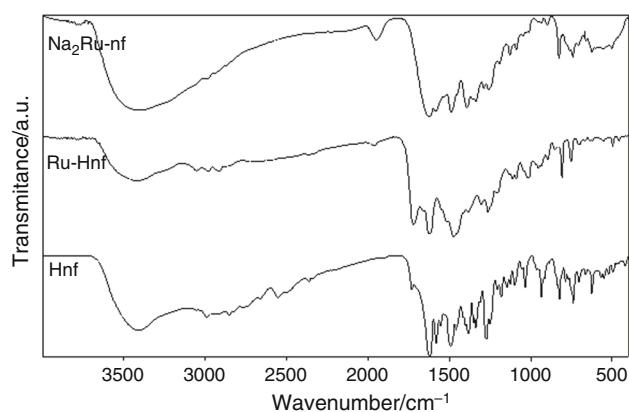
IR spectra

An important information concerning the coordination mode of quinolone ligands in the parent Ru(III) complexes and their corresponding salts can be obtained in a first approach by comparative analysis of IR spectra of norfloxacin, its Ru(III) neutral complex and the corresponding sodium salt (Fig. 1), data presented in Table 2. IR spectrum of norfloxacin is characteristic for the zwitterionic form, having in view the very weak stretching vibration of $\nu(\text{C}=\text{O})$ carboxylic at 1731 cm^{-1} due to moving of carboxylic hydrogen to the terminal piperazinyl nitrogen atom [14]. The two bands at 1580 and 1380 cm^{-1} are assigned to asymmetric and the symmetric stretching of the deprotonated carboxylate group, respectively [15], while the very strong band at 1621 cm^{-1} is due to the stretching vibration of the $\nu(\text{C}=\text{O})$ pyridone. In the neutral complex $[\text{RuCl}_3(\text{Hnf})_2(\text{DMSO})] \cdot \text{H}_2\text{O}$ norfloxacin acts as unidentate ligand [12] coordinated through N⁴(piperazyl) atom. As consequence, the vibration of $\nu(\text{C}=\text{O})$ carboxylic from protonated carboxyl group gives a very strong band in the IR spectrum. The stretching vibration of the $\nu(\text{C}=\text{O})$ pyridine is very slightly shifted from 1621 to 1626 cm^{-1} and with unchanged intensity, suggesting that this group is not involved in coordination. The IR spectrum of the sodium salt of this complex, $\text{Na}_2[\text{RuCl}_3(\text{nf})_2(\text{DMSO})] \cdot \text{EtOH} \cdot \text{H}_2\text{O}$, has a pattern very similar to that of norfloxacin in the zwitterionic form, proving both the carboxyl group deprotonation, and that the carboxyl and carbonyl (pyridone) groups are not involved in coordination.

In the IR spectra of the sodium salt of Ru(III) complexes, the carboxyl group deprotonation is clearly evidenced through the presence of the two characteristic vibration bands of carboxylate group: $\nu_{\text{as}}(\text{COO}^-)$ around 1585 cm^{-1} and $\nu_{\text{s}}(\text{COO}^-)$ around 1390 cm^{-1} (Table 3). The values of $\Delta\nu$ are the criteria that can be used to distinguish between the binding states of the carboxylate group: (i) $\Delta\nu > 200\text{ cm}^{-1}$ was found in case of unidentate

Table 1 Proposed formulae of complexes (1)–(7)

Compound	X1	X2	R1	R2	R3	m	n	p
$\text{Na}_2[\text{RuCl}_3(\text{pip})_2(\text{DMSO})]\cdot\text{EtOH}$ (Hpip = pipemidic acid) (1)	N	N	C_2H_5	–	H	1	1	0
$\text{Na}_2[\text{RuCl}_3(\text{enx})_2(\text{DMSO})]\cdot\text{EtOH}\cdot 3\text{H}_2\text{O}$ (Henx = enoxacin) (2)	N	CH	C_2H_5	F	H	1	1	3
$\text{Na}_2[\text{RuCl}_3(\text{nf})_2(\text{DMSO})]\cdot\text{EtOH}\cdot\text{H}_2\text{O}$ (Hnf = norfloxacin) (3)	CH	C	C_2H_5	F	H	1	1	1
$\text{Na}_2[\text{RuCl}_3(\text{cp})_2(\text{DMSO})]\cdot\text{DMSO}\cdot 2\text{EtOH}$ (Hcp = ciprofloxacin) (4)	CH	C		F	H	2	2	0
$\text{Na}_2[\text{RuCl}_3(\text{enro})_2(\text{DMSO})]\cdot 1.5\text{EtOH}$ (Henro = enrofloxacin) (5)	CH	C		F	C_2H_5	1	1.5	0
$\text{Na}_2[\text{RuCl}_3(\text{of})_2(\text{DMSO})]$ (Hof = ofloxacin) (6)	CH	C		F	CH_3	1	0	0
$\text{Na}_2[\text{RuCl}_3(\text{levof})_2(\text{DMSO})]\cdot 2\text{EtOH}$ (Hlevof = levofloxacin) (7)	CH	C		F	CH_3	1	2	0

**Fig. 1** Infrared spectra of norfloxacin (**Hnf**), $[\text{RuCl}_3(\text{Hnf})_2(\text{DMSO})]\cdot\text{H}_2\text{O}$ (**Ru-Hnf**) and $\text{Na}_2[\text{RuCl}_3(\text{nf})_2(\text{DMSO})]\cdot\text{EtOH}\cdot\text{H}_2\text{O}$ (**Na₂Ru-nf**)

carboxylato complexes, (ii) $\Delta\nu < 100\text{ cm}^{-1}$ is characteristic for bidentate or chelating carboxylato complexes, and finally, (iii) $\Delta\nu \sim 150\text{ cm}^{-1}$ indicates bridging complexes that show $\Delta\nu$ comparable to ionic values [16]. As a result, the $\Delta\nu$ values [$\nu_{\text{as}}(\text{COO}^-) - \nu_{\text{s}}(\text{COO}^-)$] ranging between 190 and 205 cm^{-1} suggest in this case the presence of uncoordinated carboxylate group.

UV–Vis spectra

The formation of the sodium salts was also confirmed by UV–Vis spectra. By comparative analysis of the electronic

spectra of norfloxacin, its Ru(III) neutral and anionic complexes (Fig. 2; Table 3); it can be observed that free norfloxacin has two distinct absorption bands. The first one at 280 nm may be attributed to $\pi \rightarrow \pi^*$ transition of the heterocyclic moiety and benzene ring, respectively. The second band observed at 330 nm is attributed to $n \rightarrow \pi^*$ intraligand transition. In the spectra of Ru(III) neutral complex and the corresponding sodium salt, the first band is unchanged, and this reflects that aromatic group is not involved in the coordination. The second band is slightly shifted (5 nm) in the spectra of Ru(III) neutral complex, suggesting either a minor modification of electronic density of the ligand upon coordination or an overlapping with a charge transfer transition. This band is strongly shifted ($\sim 16\text{ nm}$) in the spectra of the sodium complex, and this can be assigned both to carboxyl group deprotonation and to overlapping with the charge transfer transition. In the visible region of spectrum, both for Ru(III) neutral complex and its sodium salt, the broadband with the absorption maxima around 530 nm can be assigned to the spin-allowed transition ${}^2\text{T}_2 \rightarrow {}^2\text{A}_2$, ${}^2\text{T}_1$ for Ru(III) in an octahedral distorted stereochemistry [17].

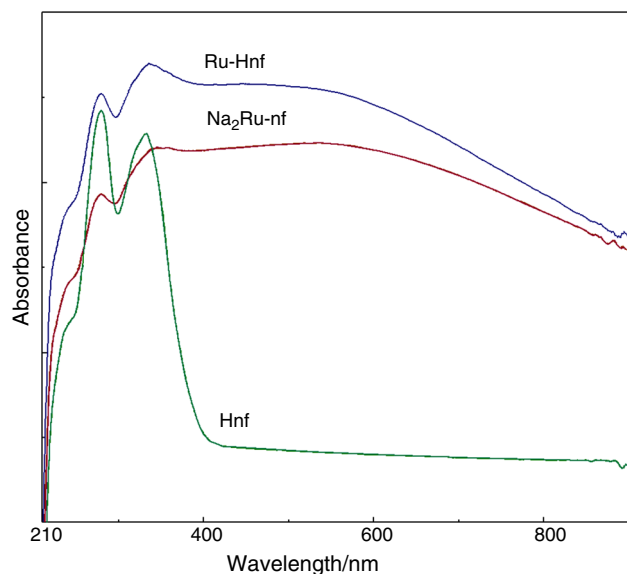
In the electronic spectra of the other sodium salts, three bands are also observed (Table 4): Two of these are placed in the UV region of electronic spectrum, between 270–290 and 336–348 nm, respectively. The third band, a broad one, with absorption maxima ranging between 450 and 540 nm is observed in the visible region of the electronic spectrum.

Table 2 Selected infrared bands of norfloxacin, its Ru(III) neutral complex and the corresponding sodium salt (cm^{-1})

Compound	$\nu(\text{C}=\text{O})$	$\nu(\text{C}=\text{O})$ (carbonyl)	$\nu_{\text{as}}(\text{COO})$	$\nu_{\text{s}}(\text{COO})$	$\Delta\nu = [\nu_{\text{as}}(\text{COO}) - \nu_{\text{s}}(\text{COO})]$
Norfloxacin (Hnf)	1731w	1621vs	1580s	1380s	200
$[\text{RuCl}_3(\text{Hnf})_2(\text{DMSO})]\cdot\text{H}_2\text{O}$	1721s	1626vs	–	–	–
$\text{Na}_2[\text{RuCl}_3(\text{nf})_2(\text{DMSO})]\cdot\text{EtOH}\cdot\text{H}_2\text{O}$ (3)	–	1622vs	1584s	1380m	204

Table 3 Selected infrared bands of complexes (1)–(7) (cm^{-1})

Compound	$\nu(\text{C}=\text{O})$	$\nu(\text{C}=\text{O})$ (carbonyl)	$\nu_{\text{as}}(\text{COO}^-)$	$\nu_{\text{s}}(\text{COO}^-)$	$\Delta\nu = [\nu_{\text{as}}(\text{COO}^-) - \nu_{\text{s}}(\text{COO}^-)]$
(1)	–	1633vs	1577s	1382m	195
(2)	1709sh	1630vs	1581m	1390w	191
(3)	–	1621vs	1584s	1380m	204
(4)	–	1623vs	1586m	1391m	195
(5)	–	1621vs	1585m	1392m	193
(6)	–	1621vs	1591s	1395m	196
(7)	–	1621vs	1590vs	1387m	203

**Fig. 2** Electronic spectra of norfloxacin (**Hnf**), $[\text{RuCl}_3(\text{Hnf})_2(\text{DMSO})] \cdot \text{H}_2\text{O}$ (**Ru-Hnf**) and $\text{Na}_2[\text{RuCl}_3(\text{nf})_2(\text{DMSO})] \cdot \text{C}_2\text{H}_5\text{OH} \cdot \text{H}_2\text{O}$ (**Na₂Ru-nf**)**Table 4** Absorption maxima from UV–Vis spectra of complexes (1)–(7)

Compound	λ/nm		
(1)	~ 494 (br)	346	273
(2)	~ 536 (br)	336	279
(3)	~ 536 (br)	346	270
(4)	~ 524 (br)	339	278
(5)	~ 465 (br)	343.5	277
(6)	~ 449 (br)	348	290 (sh)*
(7)	~ 476 (br)	348	291.5 (sh)

* br broad

Mass spectrometry measurements

The ESI–MS spectra performed in the positive mode ionisation confirmed the complexes formulation. Thus, the complexes spectra contain either a peak corresponding to protonated coordination sphere $[\text{RuCl}_3(\text{L})_2(\text{DMSO}) + 3\text{H}]^+$, m/z : 1005 and 1008 for complexes (5) and (6), respectively, or their adduct with DMSO: $[\text{RuCl}_3(\text{L})_2(\text{DMSO}) + 3\text{H} + \text{DMSO}]^+$, m/z : 971, 1005, 1003, 1027 and 1087 for complexes (1)–(4) and (7), respectively. Also, for some complexes were detected sodiated adducts $[\text{RuCl}_3(\text{L})_2(\text{DMSO}) + 3\text{Na}]^+$, m/z : 959, 1015, 1075 and 1075 for complexes (1), (4), (6) and (7), respectively.

Thermal analysis

Thermal analysis techniques are frequently used in order to obtain useful information concerning the composition and stability of complexes. In this way, the thermal behaviour of complexes was investigated by simultaneous TG/DTG/DTA analysis, and the final residue was identified by powder X-ray diffraction. The data are summarised in Table 5. The corresponding thermal decomposition curves for some of these complexes are represented in Figs. 3–6.

Thermal decomposition of complexes

$\text{Na}_2[\text{RuCl}_3(\text{pip})_2(\text{DMSO})] \cdot \text{EtOH}$ (1)
and $\text{Na}_2[\text{RuCl}_3(\text{enro})_2(\text{DMSO})] \cdot 1.5\text{EtOH}$ (5)

The complexes (1) and (5) lose both coordinated and uncoordinated solvent molecules in a first step which seems to be not a single one according to DTG curve (Fig. 3). This endothermic step undergoes in 71–240 °C/ 67–215 °C temperature ranges due the very low volatility of DMSO (boiling point 189 °C). This behaviour was also evidenced for another species which contain DMSO molecules [18]. The remaining product undergoes a few oxidative degradation steps (as TG, DTG and DTA curves

Table 5 Thermal behaviour data (in synthetic air atmosphere) for the complexes

Complex	Step	Thermal effect	Temperature range/°C	$\Delta m_{\text{exp}}/\%$	$\Delta m_{\text{calc}}/\%$	Process
$\text{Na}_2[\text{RuCl}_3(\text{pip})_2(\text{DMSO})]\cdot\text{EtOH}$ (1)	1.	Miscellaneous	71–240	12.4	12.6	EtOH loss
	2.	Exothermic	240–900	65.1	65.2	DMSO loss Oxidative degradation of organic component
$\text{Na}_2[\text{RuCl}_3(\text{en})_2(\text{DMSO})]\cdot\text{EtOH}\cdot 3\text{H}_2\text{O}$ (2)	1.	Residue Ru + 2NaCl Endothermic	70–125	22.5	22.2	EtOH loss
	2.	Endothermic	125–235	4.2	4.2	3H ₂ O loss
	3.	Exothermic	235–900	4.8	5.00	Oxidative degradation of organic component
$\text{Na}_2[\text{RuCl}_3(\text{nf})_2(\text{DMSO})]\cdot\text{EtOH}\cdot\text{H}_2\text{O}$ (3)	1.	Residue Ru + 2NaCl Endothermic	76–125	20.4	20.4	EtOH loss
	2.	Endothermic	125–175	4.3	4.5	H ₂ O loss
	3.	Exothermic	175–900	1.6	1.7	Oxidative degradation of organic component
$\text{Na}_2[\text{RuCl}_3(\text{cp})_2(\text{DMSO})]\cdot\text{DMSO}\cdot 2\text{EtOH}$ (4)	1.	Residue Ru + 2NaCl Endothermic	55–195	21.2	21.1	2EtOH loss
	2.	Miscellaneous	195–295	14.6	14.7	DMSO loss
	3.	Exothermic	295–900	6.8	6.7	DMSO loss
$\text{Na}_2[\text{RuCl}_3(\text{entro})_2(\text{DMSO})]\cdot 1.5\text{EtOH}$ (5)	1.	Residue Ru + 2NaCl Endothermic	67–215	59.8	59.9	Oxidative degradation of organic component
	2.	Exothermic	215–900	18.8	18.7	1.5EtOH loss
	3.	Exothermic	215–900	13.6	13.2	DMSO loss
$\text{Na}_2[\text{RuCl}_3(\text{of})_2(\text{DMSO})]$ (6)	1.	Residue Ru + 2NaCl Endothermic	70–215	67.2	67.3	Oxidative degradation of organic component
	2.	Exothermic	215–900	19.2	19.5	DMSO loss
	3.	Exothermic	215–900	7.46	7.41	Oxidative degradation of organic component
$\text{Na}_2[\text{RuCl}_3(\text{levof})_2(\text{DMSO})]\cdot 2\text{EtOH}$ (7)	1.	Residue Ru + 2NaCl Endothermic	76–140	20.79	20.71	2EtOH loss
	2.	Miscellaneous	140–245	8.2	8.1	DMSO loss
	3.	Exothermic	245–900	6.5	6.8	Oxidative degradation of organic component
$\text{Na}_2[\text{RuCl}_3(\text{nf})_2(\text{DMSO})]\cdot 2\text{EtOH}$ (8)	1.	Residue Ru + 2NaCl Endothermic	76–140	20.79	20.71	2EtOH loss
	2.	Miscellaneous	140–245	8.2	8.1	DMSO loss
	3.	Exothermic	245–900	6.5	6.8	Oxidative degradation of organic component

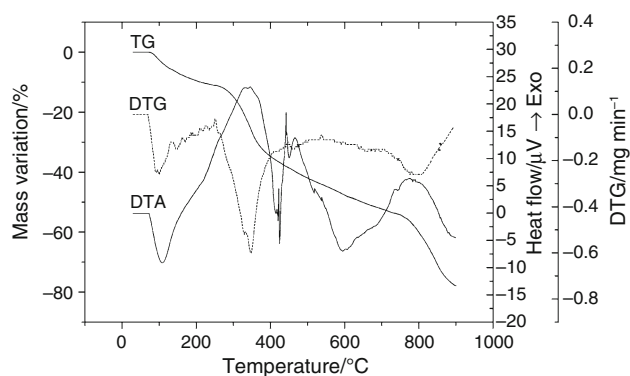


Fig. 3 TG, DTG and DTA curves of complex (1)

show) leading to the final residue which, according to powder X-ray diffraction, is a mixture of metallic ruthenium and sodium chloride (Fig. 7).

Thermal decomposition of complexes

$\text{Na}_2[\text{RuCl}_3(\text{enx})_2(\text{DMSO})] \cdot \text{EtOH} \cdot 3\text{H}_2\text{O}$ (2)

and $\text{Na}_2[\text{RuCl}_3(\text{nf})_2(\text{DMSO})] \cdot \text{EtOH} \cdot \text{H}_2\text{O}$ (3)

Thermal decomposition of complexes (2) and (3) occurs quite similar, sustaining their related formulation. The first two endothermic steps, well delimited, correspond to the ethanol molecules release in the 70–125 °C temperature range followed by the water molecules loss. This behaviour can be explained by the higher volatility of ethanol together with the lack of hydrogen bonds interaction with the complex [19]. On the other hand, it is known that the water molecules are easily involved in hydrogen bonds which explain the higher temperature needed to be released [20–22]. The intermediates without solvent molecules decompose in several overlapped steps according to TG, DTG and DTA curves (Figs. 4, 5). The final residue is also a mixture of metallic ruthenium and sodium chloride.

Thermal decomposition of complex

$\text{Na}_2[\text{RuCl}_3(\text{cp})_2(\text{DMSO})] \cdot \text{DMSO} \cdot 2\text{EtOH}$ (4)

According to TG, DTG and DTA curves, complex (4) decomposes in three well-defined steps. First, the uncoordinated solvents are released in the 55–195 °C temperature range. The next step corresponds to the coordinated DMSO molecules loss in 195–295 °C temperature range [18, 23]. Taking into account the high temperature and the miscellaneous thermal effects observed on DTA curve, we can conclude that several processes occur in this step, such as volatilisation and partial/total oxidation. The successive and well-defined release steps of DMSO molecules can be associated with the different interaction strengths involving these molecules (hydrogen interactions or coordinative bonds).

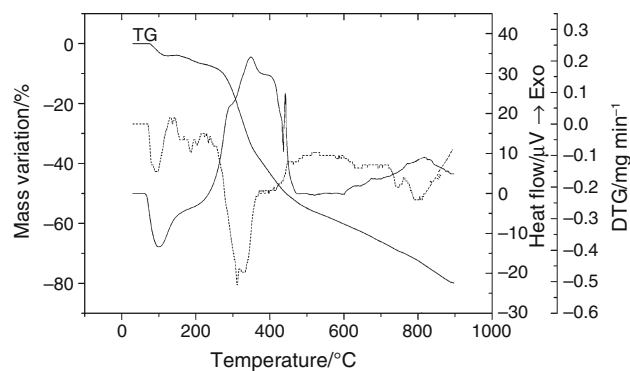


Fig. 4 TG, DTG and DTA curves of complex (2)

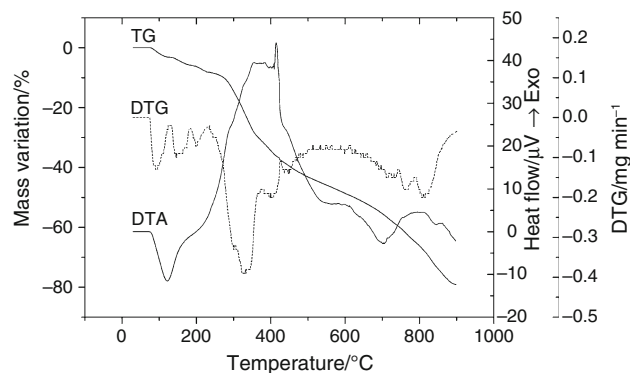


Fig. 5 TG, DTG and DTA curves of complex (3)

Over 295 °C, the remaining compound undergoes oxidative degradation leading to the same residue as previous complexes.

Thermal decomposition of complex

$\text{Na}_2[\text{RuCl}_3(\text{of})_2(\text{DMSO})]$ (6)

The $\text{Na}_2[\text{RuCl}_3(\text{of})_2(\text{DMSO})]$ complex decomposes in two steps. The first one corresponds to the DMSO loss. This is an endothermic process which occurs in 70–215 °C temperature range. The remaining product decomposes in several overlapped processes, the residue at 900 °C being the same as previous complexes.

Thermal decomposition of complex

$\text{Na}_2[\text{RuCl}_3(\text{levof})_2(\text{DMSO})] \cdot 2\text{EtOH}$ (7)

The thermal decomposition of complex (7) starts with the release of ethanol molecules, an endothermic process which occurs in 76–140 °C temperature range [19] (Fig. 6). The IR spectrum of isolated residue at 140 °C is almost identical with that of parent compound except the disappearance of band at 1055 cm^{-1} assigned to $\nu(\text{C}-\text{O})$ characteristic to primary alcohols. The next steps correspond to DMSO loss in the 140–245 °C temperature range

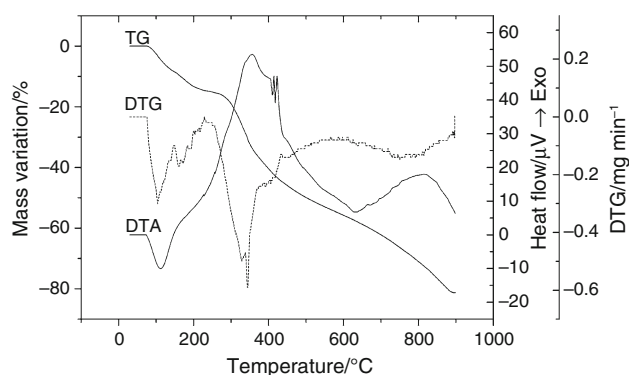


Fig. 6 TG, DTG and DTA curves of complex (7)

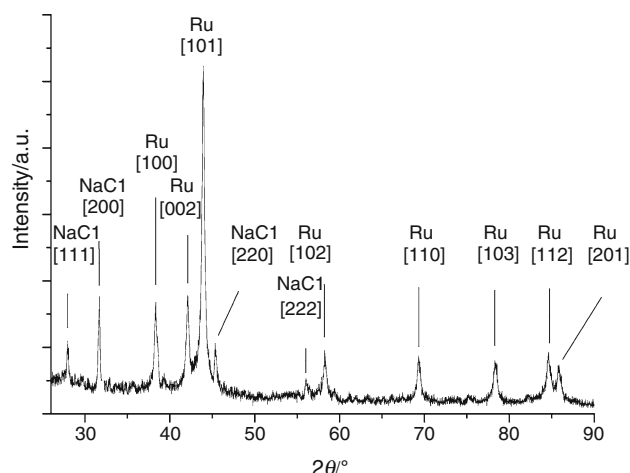


Fig. 7 Powder X-ray diffraction pattern for residue

followed by the oxidative degradation of quinolone derivative in the 245–900 °C temperature range. The DMSO loss was also confirmed by IR spectrum of isolated intermediate at 245 °C which does not exhibit the characteristic band $\nu(\text{S}=\text{O})$ at 1095 cm^{-1} unlike the parent compound.

Conclusions

In order to improve the solubility of complexes $\text{RuCl}_3(\text{HL})_2(\text{DMSO})_m(\text{H}_2\text{O})_n$ (HL: pipemidic acid, norfloxacin, ciprofloxacin, ofloxacin, levofloxacin, enrofloxacin, enoxacin), the corresponding sodium salts $\text{Na}_2\text{RuCl}_3(\text{L})_2(\text{DMSO})_m(\text{EtOH})_n(\text{H}_2\text{O})_p$ were synthesised and characterised. This pharmaceutical approach could be useful for improvement of these complexes pharmacokinetics.

The IR spectra revealed the deprotonation of carboxylate group of quinolone ligands coordinated as unidentate through $\text{N}^4(\text{piperazyl})$ atom, while the electronic spectra indicated an octahedral distorted stereochemistry.

A higher thermal stability for sodium salts was observed compared to the parent compounds as thermal analysis revealed. The decomposition of complexes occurs in two or three steps corresponding to solvent molecules (lattice or coordinated) followed by oxidative degradation of quinolone derivative. The final product of degradation consists in a mixture of metallic ruthenium and sodium chloride for all complexes.

Acknowledgements This work was supported by a grant of the Romanian National Authority for Scientific Research, CNDI—UEFISCDI, Project Number 136/2012.

References

- Sharma A, Jain CP. Techniques to enhance solubility of poorly soluble drugs: a review. *J Glob Pharma Technol.* 2010;2:8–28.
- Serajuddin ATM. Salt formation to improve drug solubility. *Adv Drug Deliv Rev.* 2007;59:603–16.
- Kratochvil B. Solid forms of pharmaceutical molecules. In: Šesták J, Mareš JJ, Hubík P, editors. *Glassy, amorphous and disordered materials: thermal physics, analysis, structure and properties.* Berlin: Springer; 2011. p. 136.
- Keller H, Keppler B. Medicament formulations containing ruthenium compounds with an antitumoral action, US Patent, 4843069, 1989.
- Kapitza S, Pongratz M, Jakupc MA, Heffeter P, Berger W, Lackinger L, Keppler BK, Marian B. Heterocyclic complexes of ruthenium(III) induce apoptosis in colorectal carcinoma cells. *J Cancer Res Clin Oncol.* 2005;131:101–10.
- Pieper T, Peti W, Sommer M, Keppler BK. Development of the tumor-inhibiting complex salt sodium *trans*-tetrachlorobis(indazole)ruthenate(III). In: Fiebi HH, Burger AM, editors. *Relevance of tumor models for anticancer drug development*, vol. 54 of: Queisser W, Scheithauer W, eds, contributions to Oncology. Basel: Karger; 1999. p. 451.
- Mestroni G, Alessio E, Sava G. New salt of anionic complexes of Ru(III) as antimetastatic and antineoplastic agents. International Patent, PCT C 07F 15/00, A61K 31/28. WO 98/00431, 1998.
- Mestroni G, Alessio E, Sava G, Pacor S, Coluccia M, Boccarelli A. Water-soluble ruthenium(III)-dimethyl sulfoxide complexes: chemical behaviour and pharmaceutical properties. *Met Based Drugs.* 1993;1:41–63.
- Sava G, Salerno G, Bergamo A, Cocchietto M, Gagliardi R, Alessio E, Mestroni G. Reduction of lung metastases by $\text{Na}[\text{trans-RuCl}_4(\text{DMSO})\text{Im}]$ is not coupled with the induction of chemical xenogenization. *Met Based Drugs.* 1996;3:67–73.
- Lentz F, Drescher A, Lindauer A, Henke M, Hilger RA, Hartinger CG, Scheulen ME, Dittrich C, Keppler BK, Jaehde U. Pharmacokinetics of a novel anticancer ruthenium complex (KP1019, FFC14A) in a phase I dose-escalation study. *Anticancer Drugs.* 2009;20:97–103.
- Rademaker-Lakhai JM, van den Bongard D, Pluim D, Beijnen JH, Schellens JHM. A phase I and pharmacological study with imidazolium-*trans*-DMSO-imidazole-tetrachlororuthenate, a novel ruthenium anticancer agent. *Clin Cancer Res.* 2004;10:3717–27.
- Badea M, Olar R, Marinescu D, Uivarosi V, Iacob D. Thermal decomposition of some biologically active complexes of ruthenium (III) with quinolone derivatives. *J Therm Anal Calorim.* 2009;97:35–739.

13. Badea M, Olar R, Marinescu D, Uivarosi V, Nicolescu TO, Iacob D. Thermal study of some new quinolone ruthenium(III) complexes with potential cytostatic activity. *J Therm Anal Calorim.* 2010;99:829–34.
14. Živec P, Perdih F, Turel I, Giester G, Psomas G. Different types of copper complexes with the quinolone antimicrobial drugs ofloxacin and norfloxacin: structure, DNA- and albumin-binding. *J Inorg Biochem.* 2012;117:35–47.
15. Turel I, Bukovec P, Quirós M. Crystal structure of ciprofloxacin hexahydrate and its characterization. *Int J Pharm.* 1997;152:59–65.
16. Refat MS. Synthesis and characterization of norfloxacin-transition metal complexes (group 11, IB): spectroscopic, thermal, kinetic measurements and biological activity. *Spectrochim Acta A.* 2007;68:1393–405.
17. Lever ABP. *Inorganic electronic spectroscopy.* Amsterdam: Elsevier; 1986. p. 454.
18. Holló B, Krstić M, Sovilj SP, Pokol G, Mészáros SK. Thermal decomposition of new ruthenium(II) complexes containing *N*-alkylphenothiazines. *J Therm Anal Calorim.* 2011;105:27–32.
19. Shah RK, Abou-Melha KS, Saad FA, Yousef T, Al-Hazmi GAA, Elghalban MG, Khedr AM, El-Metwaly N. Elaborated studies on nano-sized homo-binuclear Mn(II), Fe(III), Co(II), Ni(II), and Cu(II) complexes derived from N₂O₂ Schiff base, thermal, molecular modeling, drug-likeness, and spectral. *J Therm Anal Calorim.* 2016;123:731–43.
20. Ninković DB, Janjić GV, Zarić SD. Crystallographic and ab initio study of pyridine stacking interactions. Local nature of hydrogen bond effect in stacking interactions. *Cryst Growth Des.* 2012;12:1060–3.
21. Olar R, Vlaicu ID, Chifiriuc MC, Bleotu C, Stănică N, Scăteanu GV, Silvestro L, Dulea C, Badea M. Thermal behavior of new nickel(II) complexes with unsaturated carboxylates and heterocyclic N-donor ligands. *J Therm Anal Calorim.* 2016. doi:[10.1007/s10973-016-5445-3](https://doi.org/10.1007/s10973-016-5445-3).
22. Zarafu I, Badea M, Ioniță G, Ioniță P, Păun A, Bucur M, Chifiriuc MC, Bleotu C, Olar R. Spectral, magnetic, thermal and biological studies on Ca(II) and Cu(II) complexes with a novel crowned Schiff base. *J Therm Anal Calorim.* 2016. doi:[10.1007/s10973-016-5573-9](https://doi.org/10.1007/s10973-016-5573-9).
23. Migdał-Mikuli A, Szostak E, Drużbicki K, Dołga D. Polymorphism and thermal decomposition of [Ni(DMSO)₄]₂. *J Therm Anal Calorim.* 2008;93:853–6.